



5-5-2011

Numerical Simulation of Nonlinear Wave Propagation with Application to Geophysical Prospecting

Andrew M. Smith
Butler University

Follow this and additional works at: <http://digitalcommons.butler.edu/ugtheses>



Part of the [Physics Commons](#)

Recommended Citation

Smith, Andrew M., "Numerical Simulation of Nonlinear Wave Propagation with Application to Geophysical Prospecting" (2011).
Undergraduate Honors Thesis Collection. Paper 103.

This Thesis is brought to you for free and open access by the Undergraduate Scholarship at Digital Commons @ Butler University. It has been accepted for inclusion in Undergraduate Honors Thesis Collection by an authorized administrator of Digital Commons @ Butler University. For more information, please contact fgaede@butler.edu.

BUTLER UNIVERSITY HONORS PROGRAM

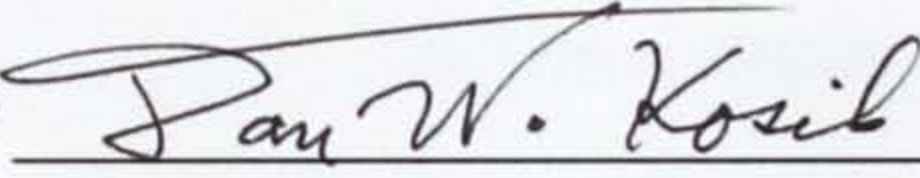
Honors Thesis Certification

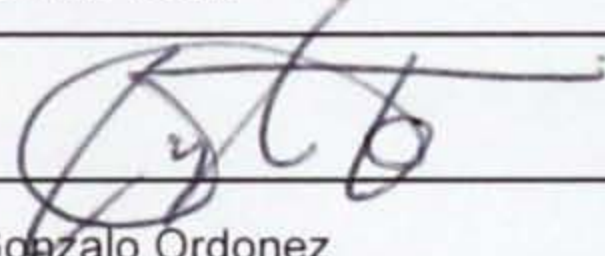
Applicant Andrew Maven Smith

Thesis title "Numerical Simulation of Nonlinear Wave Propagation with Application to Geophysical Prospecting"

Intended date of commencement May 14, 2011

Read, approved, and signed by:

Thesis adviser(s)  5/5/11
Dan W. Kosik Date

Reader(s)  5/5/11
Gonzalo Ordonez Date

Certified by  6/2/11
Director, Honors Program Date

For Honors Program use:

Level of Honors conferred: University Summa Cum Laude

Departmental Physics with Highest Honors

Mathematics with Honors

Geophysical Prospecting and the Context of this Work

Numerical Simulation of Nonlinear Wave Propagation with Application to Geophysical Prospecting

A Thesis

Presented to the Department of Physics

College of Liberal Arts and Sciences

and

The Honors Program

of

Butler University

In Partial Fulfillment

of the Requirements for Graduation Honors

Andrew M. Smith

May 5, 2011

1 Geophysical Prospecting and the Context of this Work

While the problem of simulating non-linear wave propagation can be addressed entirely within the subject of continuum mechanics, it is enlightening to begin by considering the applications of this work in the field of geophysics. In short, geophysics is the use of physical measurements to deduce the earth's interior structure. The types of measurements employed within this field range from quantifying surface displacements after a dynamite blast to examining variations in the earth's gravitational or electric field [2]. From these measurements, it is then often possible for geophysicists to predict the structure and composition of unseen geological formations underfoot.

Within the field of geophysics, geophysical prospecting is the use of geophysical procedures to locate deposits of useful materials such as oil, natural gas, and minerals. This is in contrast to geological prospecting in which scientists look directly at rock samples from exposed areas or bore holes to locate deposits. Geophysical prospecting is of particular interest today as recent decades have seen dwindling reserves of many of the fossil fuels and minerals necessary for maintaining the current state of human society. In fact, in 2011 Exxon Mobil reported that for the first time in the last 17 years it had pumped more oil than it found in new reserves—finding only 95 barrels for every 100 barrels extracted [4]. Among oil producers this is a relatively high replacement rate as most companies routinely pump more oil than they find in new reserves. Making matters worse, many experts now believe that the estimated reserves in the Middle East have been largely inflated. As materials such as oil become more

difficult to find using conventional methods, it becomes increasingly important to develop more advanced prospecting and extraction techniques.

In this vein, our work focuses on further developing one of the most commonly used techniques in geophysical prospecting—the seismic reflection method [2]. In this process, pressure pulses are produced near the earth’s surface (generally by detonating strings of dynamite). These pulses propagate downward and then are reflected back towards the surface from underlying geological formations. At the surface, displacements caused by these reflected waves are measured by instruments known as geophones. By analyzing the time of arrival and form of these reflected waves, geophysicists are able to reconstruct a map of rock layers and other relevant underground features. This information can then be used to directly predict the presence of materials of interest and guide further exploration.

Specifically, this research is intended to extend the use of the seismic reflection method to materials for which traditional linear wave analysis is insufficient. Presently prospectors using this method assume a simple linear or Hook’s law-like relation between the applied force and deformation of underlying geological materials. While this approximation is very accurate for small displacements in dense consolidated materials and bedrock, unconsolidated materials such as sand exhibit inherent non-linearity regardless of the size of deformation [6, 12]. The porous and granular nature of unconsolidated materials makes them notoriously difficult to model using analytic techniques as their behavior depends greatly on the mesoscopic properties and orientations of the individual granules. In general the relationship between applied force and deformation, also called the material’s constitutive equation, is both non-linear

and history dependent for unconsolidated materials. In other words, the relationship is complex and is not a function of only the material's current state but also of the previous states of the material.

In order to cope with these difficulties, our work uses a numerical approach when solving the problems related to seismic prospecting in areas dominated by sand and loose soil. Rather than using a closed form expression for the force-deformation relation, this work uses a model developed by McCall and Guyer[6, 12] which fits the empirical constitutive relation known as the using the P-M space method[11]. The P-M (Preisach-Mayergoyz) space model is a general model of hysteretic behavior which can be applied to numerous physical situations. Applied to unconsolidated materials, the P-M space model is based on the idea that a mesoscopic crack or pore in a material may be modeled using a highly simplified constitutive equation referred to as a hysteretic mesoscopic elastic unit (HEMU). By assembling the proper distribution of these simplified HEMUs, a constitutive relationship corresponding to real unconsolidated material emerges. Using this constructed constitutive equation, an accurate numerical solution to wave motion in unconsolidated materials can be found.

Ultimately the goal of this research is to better map geological formations beneath the Earth's surface. By using the P-M space model rather than traditional linear models for the constitutive relation, geophysicists will be able to better resolve and interpret data collected in areas where unconsolidated materials are present. With this improved knowledge of wave propagation behavior, an enhanced data inversion process may be developed—resulting in an overall increase in the quality of geological

maps. Additionally, an understanding of the dynamics of waves in unconsolidated materials will allow for improved design of source arrays when prospecting. Generally when prospecting, a number of dynamite charges are arranged in a line in the area to be surveyed and simultaneously set off as a single source. When designing a layout for these charges it is important to consider the behavior of coherent noise, or ground roll, propagated along the surface as this factor can lead to degraded measurements at the surface and large amounts of wasted blast energy. Depending on the extent of signal degradation it may become very difficult to obtain any useful results using the seismic reflection method. At the present, geophysicists attempt to address these factors within the framework of the linear wave propagation theory.

This project is aimed at addressing these aspects of source pulse array design in the context of non-linear unconsolidated materials. In accomplishing this task, the non-linear wave propagation simulation created by D.W.Kosik (in part described in [9]) was modified to accommodate multiple source charges placed at varying locations. Following this modification, computational experiments were considered for various source pulse layouts. The hope is that eventually this research will lead to array designs which will lead to significant improvements in the quality of the data extracted in a single shot and expand the number of sites yielding meaningful geophysical data to include locations where unconsolidated materials are prevalent.

As a final note, I point out that the results of our simulation could also be used to form a better understanding of materials near the earth's surface in earthquake scenarios [6]. In general, the soil most manmade structures are built upon fit into the realm of unconsolidated materials. By understanding the dynamics and the non-

linear waves produced in these materials, we can better anticipate structural behavior in the event of an earthquake and engineer buildings accordingly.

2 A Theoretical Description of the Problem

As stated before, the problem underlying wave propagation in unconsolidated materials fits into the framework of continuum mechanics. Fundamentally, the problem of many particles interacting may be addressed using the equations of motion (coupled ordinary differential equations) which result from the application of Newton's laws. While this process is useful for small or moderate collections of particles, it becomes intractable in systems where large amounts of particles are involved. For instance, a rough estimate of the number of sand grains per cubic meter is on the order of 10^{10} (clearly this will vary based on the size distribution of the sand particles). Even with the most advanced computer simulations today, such as those used in the gravitational N-body problem [8] or molecular dynamics[13], direct integration of the equations of motion becomes impractical for more than about 10^6 particles due to exponentially increasing run times.

In order to circumvent these issues, continuum mechanics chooses to treat a physical system consisting of many particles as a single continuous body. The concept of particle mass and position are replaced with density and displacement fields while Newton's equations are recast in terms of integral equations known as balance equations. In general, this sort of continuum approximation is possible whenever there is a large number of particles inside any given volume (sized according to the relevant

length scale of the problem) and groups of nearby particles more or less move together as a unit. Note the first of these conditions is equivalent to the density of the material being approximately continuous. As this research describes unconsolidated materials using this framework, a brief treatment of the basic continuum mechanics principles will be given. Namely, deformation and kinematics, the characterization of force, and constitutive (force-deformation) equations will be addressed. This presentation of the basic continuum theory (excluding the sections on the constitutive equation) is loosely based on references [5, 3, 10].

2.1 Continuum Kinematics: The Displacement Field and Measures of Strain

In particle mechanics, the basic tools used to describe the motion of a system are the position vectors \vec{r}_i . In continuum mechanics, the quantity chosen for describing a body's motion is the displacement field \vec{u} . In defining the displacement field, we first consider a reference configuration of the body at a time t_o . This snapshot of a body's motion can be taken at any time but generally is chosen at a time when the body is in equilibrium. Now to each material point within the body, a label \vec{a} is assigned corresponding to its position in the reference configuration. As time moves forward, each material point then follows a trajectory $\vec{x}_{\vec{a}}(t)$ (also denoted $\vec{x}(\vec{a}, t)$) where $\vec{x}_{\vec{a}}(0) = \vec{a}$. These trajectories are completely analogous to the position vectors \vec{r}_i in particle mechanics despite the fact the indices now form a continuum. Using

this notation, the displacement field is defined by

$$\begin{aligned}\vec{u}(\vec{a}, t) &= \vec{x}_{\vec{a}}(t) - \vec{x}_{\vec{a}}(0) \\ &= \vec{x}_{\vec{a}}(t) - \vec{a}.\end{aligned}$$

In words, the displacement field is a function which assigns each material point \vec{a} within the reference configuration a displacement vector pointing from its initial position to its current location. Note that this same system of characterizing motion could be used to describe a system of just N particles. In this case \vec{u} would be defined on only N points in space corresponding to the N particle position vectors at t_0 .

While the displacement field clearly and intuitively describes the motion of a system, it is not a useful concept when relating a body's configuration to the forces acting between its constituent particles. For instance, the forces acting within an object are unaltered after the object is translated across the room or rotated in place. Yet in each of these cases, the displacement field of the object is non-trivial. Rather than using the displacement field to describe a body's configuration, it would be ideal to have a function which identifies stretching within a body as these changes correspond to changing forces. In particle mechanics this is analogous to the fact that particle interactions do not depend directly on the position vectors \vec{r}_i but rather on displacements of the form $\vec{r}'_i - \vec{r}_i$.

Trying to take this exact idea from particle mechanics and create a function $d(\vec{a}, \vec{a}', t)$ which gives the distance between any two material points \vec{a} and \vec{a}' at time t would be very challenging. In general such a function would be highly non-linear

and hence difficult to work with. Luckily the interactions in continuum mechanics are due to short range forces which result from the direct contact of mesoscopic particles or microscopic interactions within a body. As a consequence, we need only look at changes in the distance between a material point and its close neighbors. More specifically, we hope to find a field of functions $C_{(\vec{a},t)}$ which can accomplish this goal. Consider a material point \vec{a} with close neighbors \vec{a}_i where $i = 1, 2$. Define the vectors

$$\begin{aligned}\vec{s}_i &= \vec{a}_i - \vec{a} \\ &= \vec{x}_{\vec{a}_i}(0) - \vec{x}_{\vec{a}}(0) \\ \vec{s}'_i &= \vec{x}_{\vec{a}_i}(t) - \vec{x}_{\vec{a}}(t).\end{aligned}$$

Observe the dot product

$$\begin{aligned}\vec{s}'_1 \cdot \vec{s}'_2 &\approx \nabla \vec{u}|_{(\vec{a},t)}(\vec{s}_1) \cdot \nabla \vec{u}|_{(\vec{a},t)}(\vec{s}_2) \\ &= [\vec{s}_1]^T [\nabla \vec{u}|_{(\vec{a},t)}]^T [\nabla \vec{u}|_{(\vec{a},t)}] [\vec{s}_2].\end{aligned}$$

Note that in the limit of $|\vec{s}_i| \rightarrow 0$ this approximation becomes equality which follows with our assumptions that the three points all be in a small neighborhood. Thus one manifestation of the desired local distance function $C_{(\vec{a},t)}$ is the field of bilinear forms defined by the equation

$$\begin{aligned}C_{(\vec{a},t)}(\vec{s}_i, \vec{s}_i) &= [\vec{s}_i]^T [\nabla \vec{u}|_{(\vec{a},t)}]^T [\nabla \vec{u}|_{(\vec{a},t)}] [\vec{s}_i] \\ &= \|\vec{s}'_i\|^2.\end{aligned}$$

In continuum mechanics this object is called the Cauchy–Green strain tensor (hence the preemptive naming). Those who are familiar with differential geometry will recognize the Cauchy–Green Strain tensor to be nothing more than the metric tensor or first fundamental form. It is a function field which takes two displacement vectors from the material point \vec{a} at time t_0 and gives the dot product of the corresponding displacement vectors at time t . Moreover it is just one of the many functions which characterizes the deformation of a body. Such a function is called a measure of strain.

Another useful measure of strain is the Lagrangian strain tensor defined by

$$\begin{aligned}
 E_{(\vec{a},t)}(\vec{s}_i, \vec{s}_i) &= \frac{1}{2} \left(C_{(\vec{a},t)}(\vec{s}_i, \vec{s}_i) - \vec{s}_i \cdot \vec{s}_i \right) \\
 &= \frac{1}{2} [\vec{s}_i]^T [\nabla \vec{u}|_{(\vec{a},t)} - I]^T [\nabla \vec{u}|_{(\vec{a},t)} - I] [\vec{s}_i] \\
 &= \frac{1}{2} [\vec{s}_i]^T \left([\nabla \vec{u}|_{(\vec{a},t)}] + [\nabla \vec{u}|_{(\vec{a},t)}]^T + [\nabla \vec{u}|_{(\vec{a},t)}]^T [\nabla \vec{u}|_{(\vec{a},t)}] \right) [\vec{s}_i] \\
 &= \frac{1}{2} (\|\vec{s}'_i\|^2 - \|\vec{s}_i\|^2).
 \end{aligned}$$

Specifically, consider the limit of the Lagrangian strain tensor in which the particles in a body are displaced only very slightly. In the limit that these displacements go to zero, the displacement field $\vec{u}_{\vec{a}}(t)$ and therefore the deformation gradient $\nabla \vec{u}_{\vec{a}}|_t$ approach zero. Ignoring the second order term due to the product of gradients, the Lagrangian strain measure then reduces to the so called infinitesimal strain tensor

$$\begin{aligned}
 \varepsilon_{(\vec{a},t)}(\vec{s}_i, \vec{s}_i) &= \frac{1}{2} [\vec{s}_i]^T \left([\nabla \vec{u}|_{(\vec{a},t)}] + [\nabla \vec{u}|_{(\vec{a},t)}]^T \right) [\vec{s}_i] \\
 &\approx \frac{1}{2} (\|\vec{s}'_i\|^2 - \|\vec{s}_i\|^2)
 \end{aligned}$$

This strain measure is of particular importance to the work that follows. To see why consider two material points separated by a small amount in the x direction (i.e. $\vec{s} = \hat{x}\Delta x$). In this case it follows that

$$\begin{aligned} \|\vec{s}'\|^2 - \|\vec{s}\|^2 &= (\|\vec{s}'\| - \|\vec{s}\|)(\|\vec{s}'\| + \|\vec{s}\|) \\ &\approx 2\varepsilon_{(a,t)}(\vec{s}, \vec{s}) \\ &= 2\varepsilon_{xx}(\Delta x)^2 \end{aligned}$$

From the fact that the deformation gradient goes to zero, we may make the additional approximation that $\|\vec{s}'\| \approx \|\vec{s}\|$. It follows that the fractional length change in the x direction is equal to ε_{xx} .

$$\begin{aligned} \frac{\|\vec{s}'\| - \|\vec{s}\|}{\|\vec{s}\|} &= \frac{2\varepsilon_{xx}(\Delta x)^2}{\|\vec{s}\|(\|\vec{s}'\| + \|\vec{s}\|)} \\ &\approx \frac{2\varepsilon_{xx}(\Delta x)^2}{\Delta x(2\Delta x)} \\ &= \varepsilon_{xx}. \end{aligned}$$

This fractional measure of length changes will be especially useful in relating the deformation of a body to the continuum mechanics notion of force called stress. For instance, consider a string which is stretched by some small amount. In this case the relevant quantity in determining the tension is not the net length change but rather the fractional change in the string's length. Clearly when a short string and a long string are stretched by the same amount the tension in the shorter string is much larger! The other components of the infinitesimal strain tensor have similar

interpretations. Particularly, the off diagonal terms of the strain tensor, called the shear terms, may be related to fractional changes in the angle between the unit vectors corresponding to its indices. This is not surprising considering the relationship of the strain tensor to the dot product.

With this, our discussion of strain is concluded. Note that for the remainder of this work, the strain fields will generally be referred to without the subscripts which refer to the field point except for when the field point is not clear from context. Also no distinction will be made between the bilinear strain functions and their matrix representations.

2.2 Continuum Dynamics: Force, Stress, and the Momentum Balance Equation

In the last section, methods for describing the kinematics—the motion and deformation—of a continuous body were developed. The current section has two main objectives. Firstly, the concept of force will be extended into the domain of continuum mechanics through the concept of strain. Secondly, the correct generalization of Newton's second law for continuous bodies will be developed, in effect creating a relationship between the physical notions of force and mass to the kinematic aspects of a body.

To begin, consider a material body and, within this body, choose any volume V bounded by the surface ∂V . Now consider the total force acting on the region V . In general this force may be decomposed into a surface term and a volume term.

Mathematically this is encompassed by the equation

$$\begin{aligned}\vec{F} &= \vec{F}_{\partial V} + \vec{F}_V \\ &= \int_{\partial V} \vec{T}_{\hat{n}}(\vec{x}, t) dA + \int_V \vec{B}(\vec{x}, t) dV\end{aligned}$$

where $\vec{T}_{\hat{n}}$ is the (vector) force per unit area acting on a surface element perpendicular to \hat{n} while \vec{B} is the force per unit volume acting on V . Respectively, the quantities $\vec{T}_{\hat{n}}$ and \vec{B} are called the traction and body force. In general, traction represents both the effects of short range forces and direct collisions between particles. In contrast, the body force is due to entities which act at longer distances such as the gravitational or electromagnetic field. As this work is concerned only with contact forces, the following discussion will focus on traction and assume the absence of body forces. Additionally in what follows, time dependence is assumed although it will not be explicitly shown.

To begin, let it be postulated that $\vec{T}_{\hat{n}} = \vec{T}_{\hat{n}}(\hat{n}, \vec{x})$. In other words, the traction field is solely a function of the position and orientation of the area element in question. Note that this excludes the possibility that traction be a function of the curvature of the surface ∂V as this would be related to derivatives of the normal field \hat{n} . Using this assumption it can be shown that

$$\vec{T}_{\hat{n}}(\hat{n}, \vec{x}) = \sigma_{\vec{x}} \cdot \hat{n}$$

where $\sigma_{\vec{x}}$ is a field of linear transformations called the stress tensor field. The above equation is attributed to Cauchy and accordingly called the Cauchy stress relation.

In words, the strain tensor at a point \vec{x} can be thought of as a matrix which when applied to the unit normal of the surface element in question produces the force per unit area. If it is further assumed that the moment of the force (torque) per unit area on a surface of diminishing size vanishes, then the $\sigma_{\vec{x}}$ becomes a symmetric tensor.

With the concept of stress in hand, the continuum generalization of Newton's second law, called the momentum balance equation, will now be developed. To do so, consider a material body and a collection of material points contained within the body. Now at any given time, this group of particles can be found in a volume $V(t)$ which changes as the material points move. For this group of particles, Newton's second law must hold and the time derivative of the integral of the momentum density must be equal to the total force on the body. This can be written

$$\begin{aligned}\vec{F} &= \frac{d}{dt} \int_{V(t)} \vec{\mathcal{P}}(\vec{x}, t) dV \\ &= \frac{d}{dt} \int_{V(t)} \rho(\vec{x}, t) \vec{v}(\vec{x}, t) dV.\end{aligned}$$

Note that the domain of the integral is time dependent and the time derivative may not enter the integral in the normal way. To overcome this issue, consider the i th component of the force. In this case

$$\begin{aligned}F_i &= \frac{d}{dt} \int_{V(t)} \mathcal{P}_i(\vec{x}, t) dV \\ &= \lim_{\Delta t \rightarrow 0} \frac{1}{\Delta t} \left[\int_{V(t+\Delta t)} \mathcal{P}_i(\vec{x}, t + \Delta t) dV - \int_{V(t)} \mathcal{P}_i(\vec{x}, t) dV \right] \\ &= \lim_{\Delta t \rightarrow 0} \frac{1}{\Delta t} \left[\int_{V(t)} \mathcal{P}_i(\vec{x}, t + \Delta t) dV + \int_{\partial V(t)} \mathcal{P}_i(\vec{x}, t) (\vec{v}(\vec{x}, t) \Delta t) \cdot d\vec{A} - \int_{V(t)} \mathcal{P}_i(\vec{x}, t) dV \right].\end{aligned}$$

The surface term can be thought of as a correction to the approximation $V(t + \Delta t) \approx V(t)$ in the first term of the previous line. Conceptually, as the material points move through space they sweep out a very thin volume around the surface $V(t)$. In the case that the particles move away from the volume $V(t)$ the quantity $(\vec{v}\Delta t) \cdot d\vec{A}$ represents a new volume added to the integral and is positive. Likewise, when the particles at the edge of $V(t)$ move into the interior of the volume, the volume is lost and a negative correction is made. By virtue of the divergence theorem, it follows

$$\begin{aligned} F_i &= \lim_{\Delta t \rightarrow 0} \frac{1}{\Delta t} \left[\int_{V(t)} \mathcal{P}_i(\vec{x}, t + \Delta t) - \mathcal{P}_i(\vec{x}, t) + \nabla \cdot \{ \mathcal{P}_i(\vec{x}, t) \vec{v}(\vec{x}, t) \Delta t \} dV \right] \\ &= \int_{V(t)} \frac{\partial \mathcal{P}_i}{\partial t}(\vec{x}, t) + \nabla \cdot \{ \mathcal{P}_i(\vec{x}, t) \vec{v}(\vec{x}, t) \} dV \end{aligned}$$

This is the desired momentum balance equation in integral form. While this equation seems like a set of three equations (one for each component of force) it actually encompasses a set of infinitely many equations as the volume $V(t)$ is arbitrary. Using this fact, the equation

$$\begin{aligned} F_i &= \int_{V(t)} \frac{\partial \mathcal{P}_i}{\partial t}(\vec{x}, t) + \nabla \cdot \{ \mathcal{P}_i(\vec{x}, t) \vec{v}(\vec{x}, t) \} dV \\ &= \int_{\partial V(t)} T_i(\vec{x}, t) dA \\ &= \left[\int_{\partial V(t)} \vec{\sigma} \cdot d\vec{A} \right]_i \\ &= \left[\int_{V(t)} \nabla \cdot \vec{\sigma} dV \right]_i \end{aligned}$$

can be reduced to the partial differential equation

$$\frac{\partial \mathcal{P}_i}{\partial t}(\vec{x}, t) + \nabla \cdot \{ \mathcal{P}_i(\vec{x}, t) \vec{v}(\vec{x}, t) \} = (\nabla \cdot \overleftrightarrow{\sigma})_i.$$

The local statement of the momentum balance equation is most useful when written in terms of density, velocity, and the stress tensor. Substituting $\mathcal{P}_i = \rho v_i$ the right hand side of the previous equation becomes

$$\begin{aligned} \frac{\partial}{\partial t}(\rho v_i) + \nabla \cdot \{ \rho v_i \vec{v} \} &= v_i \left(\frac{\partial \rho}{\partial t} + \nabla \cdot \{ \rho \vec{v} \} \right) + \rho \left(\frac{\partial v_i}{\partial t} + \vec{v} \cdot \nabla v_i \right) \\ &= \rho \left(\frac{\partial v_i}{\partial t} + \vec{v} \cdot \nabla v_i \right) \end{aligned}$$

where the first term vanishes due to the continuity equation related to conservation of mass. Replacing ∇v_i with the full Jacobian, the coordinate free local momentum balance equation takes its final form

$$\rho \left(\frac{\partial \vec{v}}{\partial t} + \nabla \vec{v} \cdot \vec{v} \right) = \nabla \cdot \overleftrightarrow{\sigma}.$$

In terms of the standard coordinate basis this equation can alternately be written

$$\rho \left(\frac{\partial v_i}{\partial t} + v_j \frac{\partial v_i}{\partial x_j} \right) = \frac{\partial \sigma_{ij}}{\partial x_j}.$$

At this point, we are almost ready to describe the motion of the displacement field.

The velocity terms in the above can in principle be replaced with terms relating to

the displacement field via the relationship

$$\vec{v} = \frac{\partial \vec{u}}{\partial t} + \nabla \vec{u} \cdot \vec{v}.$$

The relationship between stress and the displacement field is more complicated. In general, stress is related to the displacement field by a material dependent constraint called the constitutive equation which will be developed in the next section.

2.3 The Constitutive Equation: Describing the Relationship Between Stress and Strain

In this section, a constitutive equation, or material dependent stress relation, for unconsolidated materials will be developed. While the balance equation of the previous section corresponded to Newton's second law in particle mechanics, the constitutive relation is analogous to specific force laws such as the Lorentz force law or the Newtonian expression for gravity. In essence these equations relate the abstract notion of stress and force back to concrete kinematic descriptions of a body.

In general it has been found that almost all materials have a range of deformations in which the constitutive equation takes on the form

$$\sigma_{ij} = \sigma_{ij}(\varepsilon_{ij}).$$

In the case that a material's stress is purely a function of the strain tensor, we call the material elastic. Perhaps the simplest elastic constitutive equation is that of linear

elasticity

$$\sigma_{ij} = b_{ijkl}\epsilon_{kl}$$

where b_{ijkl} is a fourth order tensor which generally varies based on position. In words, the above relation states that at every material point the stress tensor elements are linear functions of the strain tensor at that point.

Unfortunately when dealing with unconsolidated materials, these simple constitutive relations are inadequate. Even for small stresses, the constitutive equations for unconsolidated materials exhibit both non-linear and anelastic behavior. For this work it will be assumed that the constitutive equation has the form

$$\sigma_{ij} = \sigma_{ij}(\epsilon_{ij}, \mathcal{I})$$

where \mathcal{I} is a field associated with the internal configuration of each material point. More specifically, this internal configuration can be associated with the state of the pores and cracks found in the vicinity of a material point. If it is further assumed that \mathcal{I} is rotation invariant, the constitutive equation for an isotropic material can be shown [9, 14] to have the form

$$\sigma_{ij} = e_0\delta_{ij} + e_1\epsilon_{ij} + e_2\epsilon_{ik}\epsilon_{kj}$$

where the scalar coefficients e_i are functions of both the strain tensor and the internal configuration of the material point. When written in terms of longitudinal, transverse,

and shear strain components, the above equation is further reduced to the form [1]

$$\sigma_{ij} = (\alpha - \beta - \gamma)\delta_{lm}\epsilon_{ij} + \beta\delta_{ij}\epsilon_{kk} + \gamma\epsilon_{ij} + \eta(\epsilon_{kk}\epsilon_{nn} - \epsilon_{kk}^2).$$

In the above α , β , γ , and η are respectively the longitudinal, transverse, shear, and longitudinal-transverse stress-strain moduli. As before these moduli are functions of the material's internal configuration \mathcal{I} . For the amplitudes expected in our simulation, the second order terms in strain may be ignored giving the final constitutive equation

$$\sigma_{ij} = (\alpha - \beta - \gamma)\delta_{lm}\epsilon_{ij} + \beta\delta_{ij}\epsilon_{kk} + \gamma\epsilon_{ij}.$$

Note that the non-linear, anelastic, and hysteretic properties of the above equation are due to the dependence of the α and β coefficients on the material's internal state \mathcal{I} . In our work it is assumed that γ is approximately constant because the shear strains are much smaller than the other strains involved. Additionally, the quantity $(\alpha - \beta - \gamma)$ is taken to be approximately zero due to the quasi-linear nature of our material. This approximation becomes exact in the linear limit. Inserting this constitutive equation into the momentum balance equation and assuming small magnitudes for the displacement field, the two dimensional wave equation for non-linear anelastic

materials is obtained [1].

$$\rho \frac{\partial^2 u_x}{\partial t^2} = \frac{\partial}{\partial x} \left[\beta \left(\frac{\partial u_x}{\partial x} + \frac{\partial u_z}{\partial x} \right) + \gamma \frac{\partial u_x}{\partial x} \right] + \frac{\partial}{\partial z} \left[\frac{\gamma}{2} \left(\frac{\partial u_z}{\partial x} + \frac{\partial u_x}{\partial z} \right) \right]$$

$$\rho \frac{\partial^2 u_z}{\partial t^2} = \frac{\partial}{\partial z} \left[\beta \left(\frac{\partial u_x}{\partial x} + \frac{\partial u_z}{\partial x} \right) + \gamma \frac{\partial u_z}{\partial z} \right] + \frac{\partial}{\partial x} \left[\frac{\gamma}{2} \left(\frac{\partial u_z}{\partial x} + \frac{\partial u_x}{\partial z} \right) \right]$$

At this point, the motion of the displacement field is completely described assuming that the dynamics of the internal state \mathcal{I} and dependence of the moduli α, β on \mathcal{I} are known. In this work these variables are determined within the confines of the P-M space model which will be discussed in the next section.

2.4 The P-M Space Model and a Realistic Hysteretic Relation Between Stress and Strain

The basis of the Preisach-Mayergoyz space model [12, 7, 6] is the idea that each material point in a body has structure on the mesoscopic scale. In reality, a body is riddled with numerous pores, cracks, and voids which expand or contract based on the stresses applied to the body. On a qualitative level, the P-M space model assumes each material point contains a large number of such defects and furthermore that the internal configuration \mathcal{I} is based on the states of these defects.

Like most materials, unconsolidated materials experience increasing (decreasing) strain with increasing (decreasing) stress. What makes these materials exotic and hysteretic is the fact that the rate at which strain increases or decreases is depen-

dent on whether stress is increasing or decreasing. For most materials, a increase in pressure by an amount ΔP will result in a corresponding change in strain $\Delta \varepsilon_1$ while the corresponding decrease $-\Delta P$ will cause a change in strain $\Delta \varepsilon_2 = -\Delta \varepsilon_1$. In unconsolidated materials, there is a delay in the decompression of the material. These materials retain heightened stress despite a decrease in pressure and hence $\Delta \varepsilon_1 > \Delta \varepsilon_2$.

In order to describe the internal state \mathcal{I} of a material point, we first construct a model for a single defect which reflects this fundamental property. To do so, a two state system called a HMEU (hysteretic mesoscopic elastic unit) which can be in either an "open" or "closed" state will be associated with each defect. Each state is assigned a characteristic length l_o, l_c and critical pressure P_o, P_c . The dynamics of the system are given as follows. A defect in the open state l_o will transition to the closed state l_c when the pressure on the system is increased past the threshold pressure P_c . Likewise the system will move from the closed state l_c to the open state l_o when the stress on the system is decreased past the opening threshold P_o . The resulting relation between length (strain) and pressure (stress) is schematically shown in the following diagram [12].

While this relationship may not closely model the material as a whole, a distribution of such elements can be assembled such that the cumulative relationship between stress and strain closely mimics that of real materials. For the purpose of this work, all HMEUs will be assumed to have the same lengths l_o and l_c and will differ solely on their pressure thresholds P_o, P_c . The distribution of HMEUs can be thought of as a set of points in the plane with axis P_o and P_c . A typical P-M space distribution in

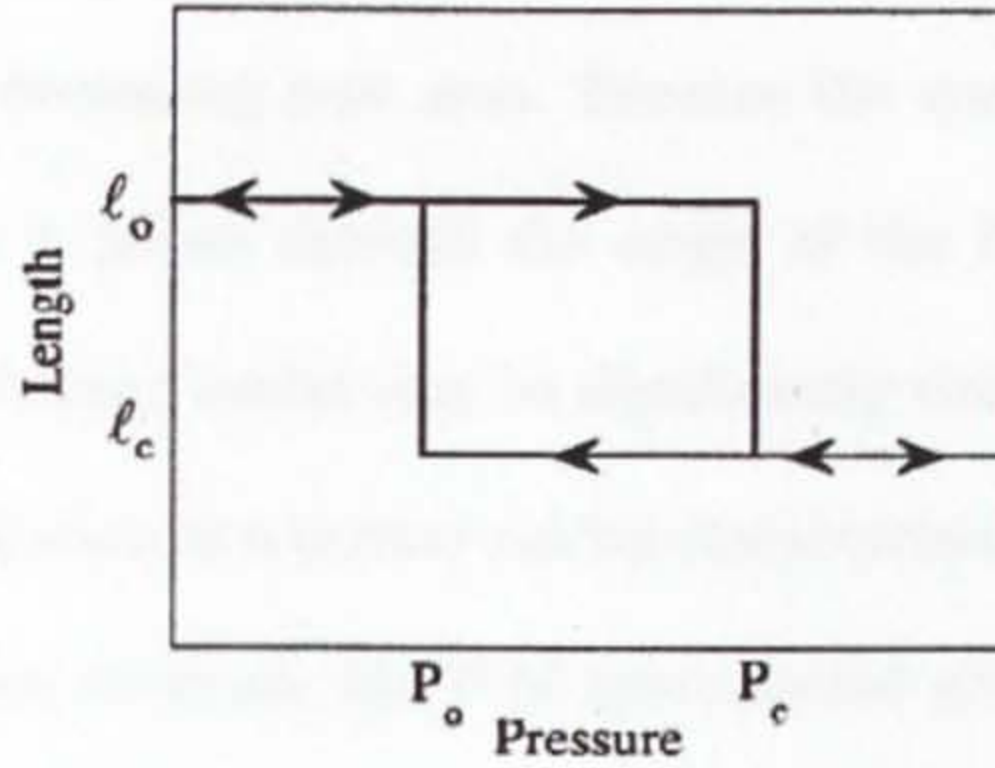


Figure 1: The hysteretic relation corresponding to a single HMEU.

units of kPa is given in the following figure[12].

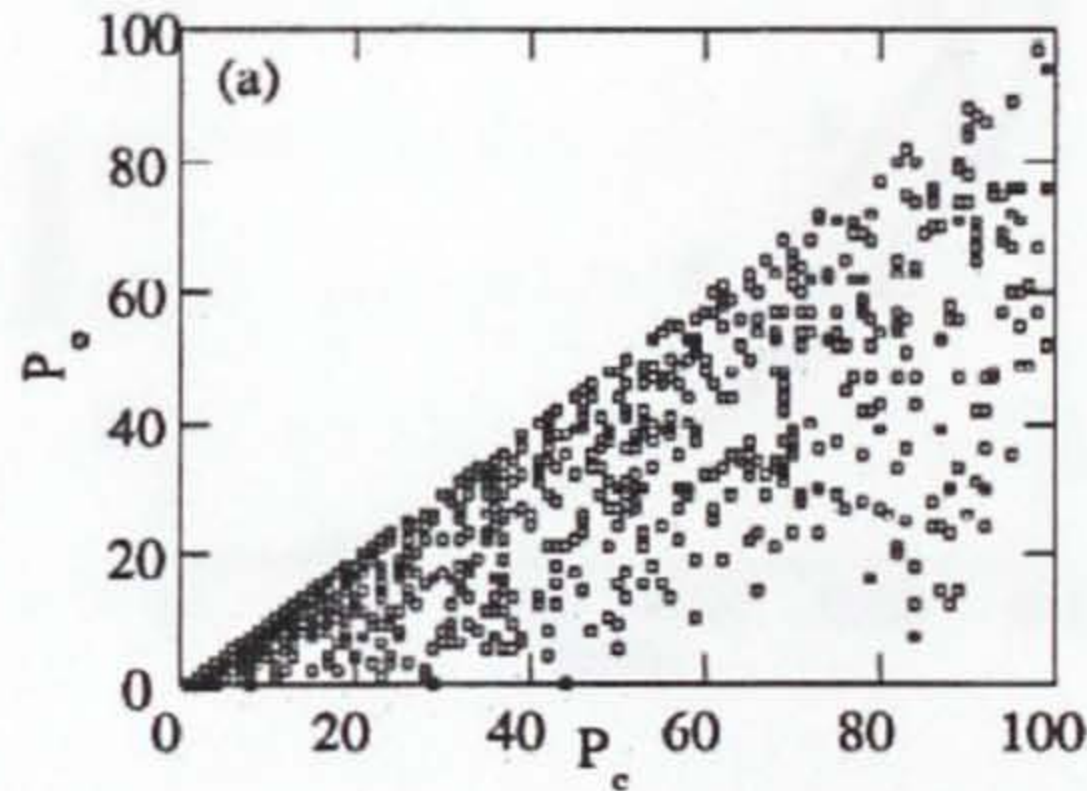


Figure 2: A sample distribution of HMEUs in P-M space.

For each material point, the internal state \mathcal{I} is then characterized by the subset of this plane which is in the closed position or, equivalently, knowledge of which HMEUs are open and which are closed.

Now in general, an arbitrary series of stressing and de-stressing a material can cause a nontrivial subset of the P-M space to become closed. For our model the situation is greatly simplified by the fact that the solutions to the wave equation

always correspond to stresses which increase monotonically to a maximum stress before monotonically decreasing past zero. Because the system effectively "forgets" its history every time it passes through the origin of the P-M space, the resulting description of the P-M space model may be significantly simplified for our model. In particular, the internal state of a system can be characterized by the maximum stress alone. For each increase in stress, the P-M space model gives the same curve while the curve associated with decreasing stress is parameterized by the maximum strain. The resulting family of curves is exemplified in the following figure[12]. To further

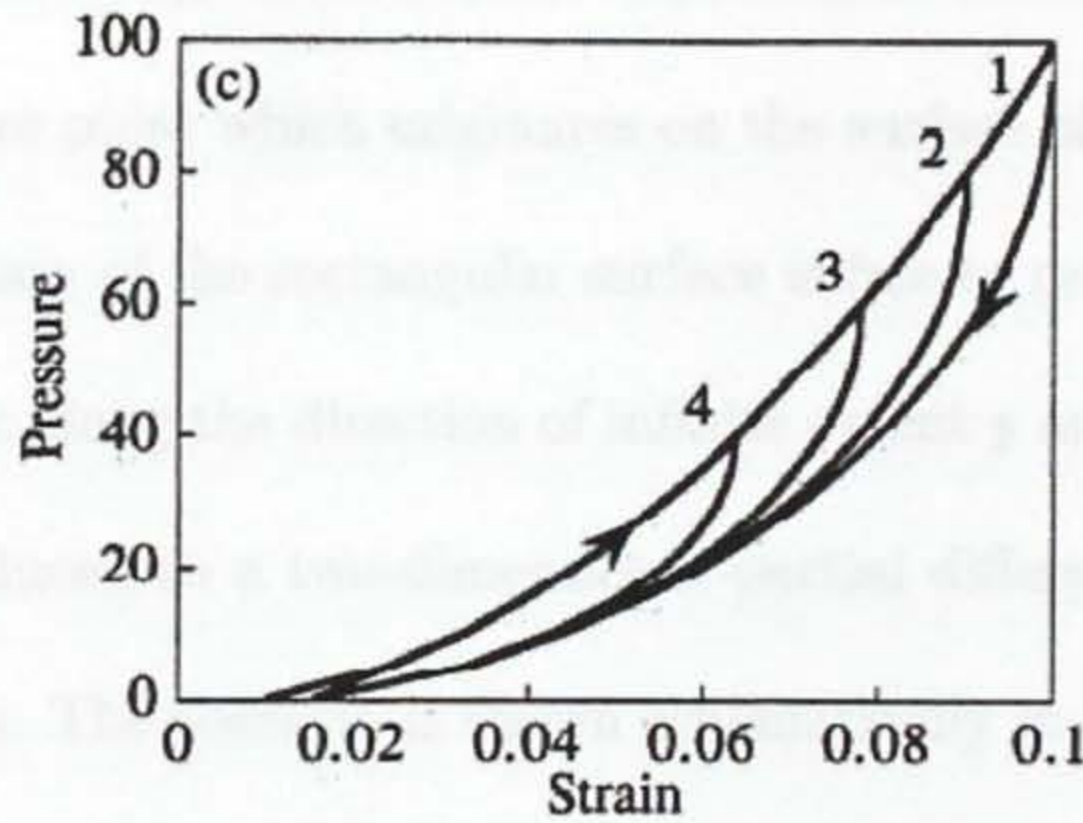


Figure 3: Family of curves resembling those produced in our simulation.

simplify matters, our code takes advantage of the fact that these decreasing stress curves are very similar in shape and uses a scaling argument to obtain all information from a single maximal stress relation.

3 The Simulation of Non-linear Anelastic Waves from a Cylindrical Source

On a qualitative level the simulation used in this work models the detonation of a long string of dynamite buried under the earth's surface. Geophysical considerations aside, the basic problem associated with our simulation is that of solving the equations of motion for a material body which is rectangular in cross section and otherwise infinite in extent. Within this body is an infinite cylindrical cavity which is circular in cross section and punches through the material. The simulation models the propagation of a Gaussian pressure pulse which originates on the surface of the cavity and moves outward. The boundary of the rectangular surface is free to move about. Clearly the problem is symmetric along the direction of infinite extent y and hence the equations of motion can be reduced to a two-dimensional partial differential equation in only the x and z variables. The scenario is shown schematically in the following figure.

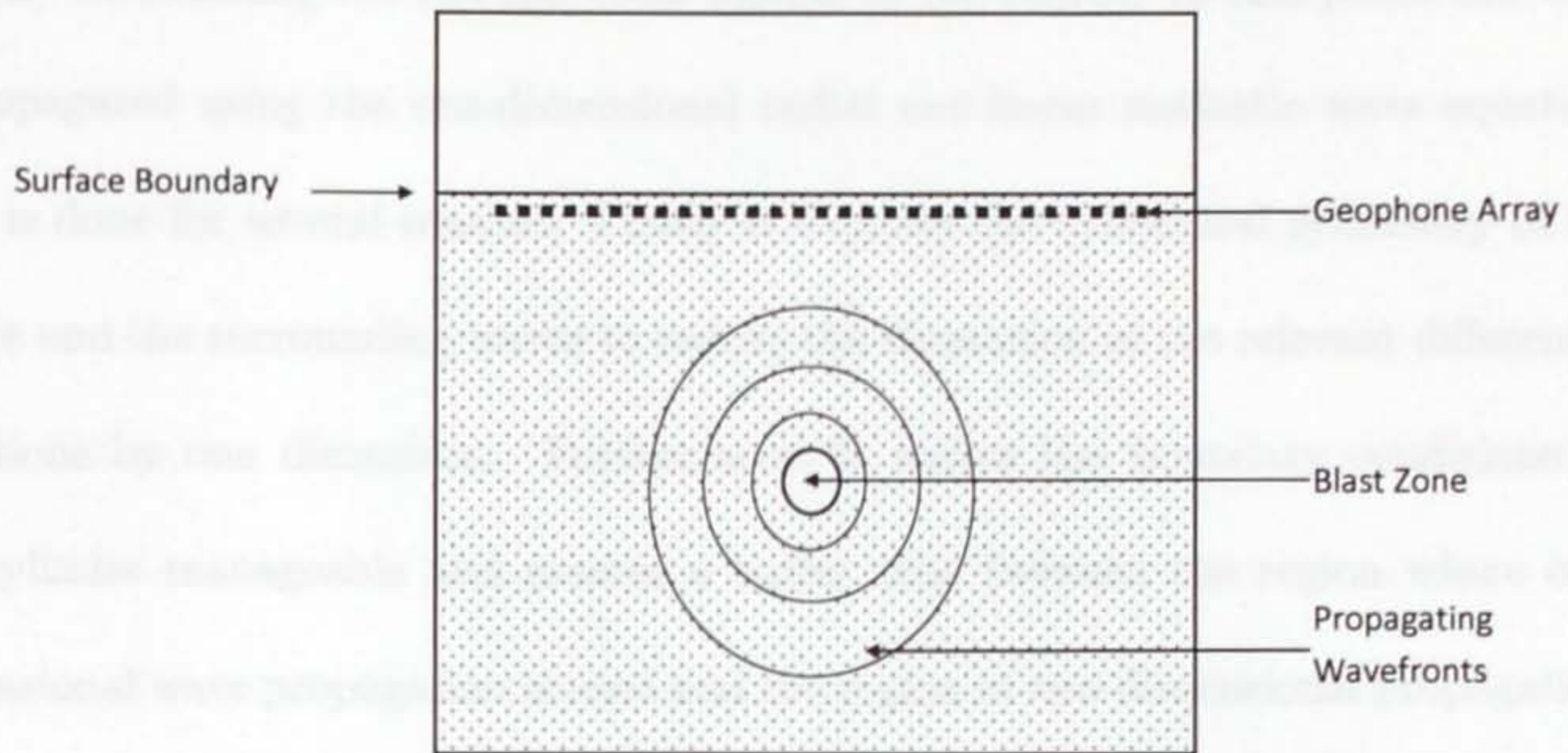


Figure 4: Cross section corresponding to simulation.

Before describing the specifics of the simulations operation, I first will give a qualitative rundown of the code's update structure. Assume that the displacement field \vec{u} , velocity field \vec{v} , and internal configuration \mathcal{I} (or equivalently α and β parameters) are known at time t . Using the given information from above, the stress field σ_{ij} can be deduced. Since the stress field is directly related to the time rate of change of the displacement field, updated velocity and displacement fields can be found for time $t + \Delta t$. Using the displacement field, the infinitesimal strain tensor ε_{ij} at time $t + \Delta t$ follows immediately. From the strain tensor and the rate of change of the strain tensor, the P-M space configuration for time $t + \Delta t$ can be calculated. At this point, all state variables are updated and a new iteration begins.

Now looking at the code in a little more depth, the primary strategy for updating the state of the system is a Crank-Nicholson iteration scheme. When calculating the updated state of the displacement field, the code begins within a small rectangular

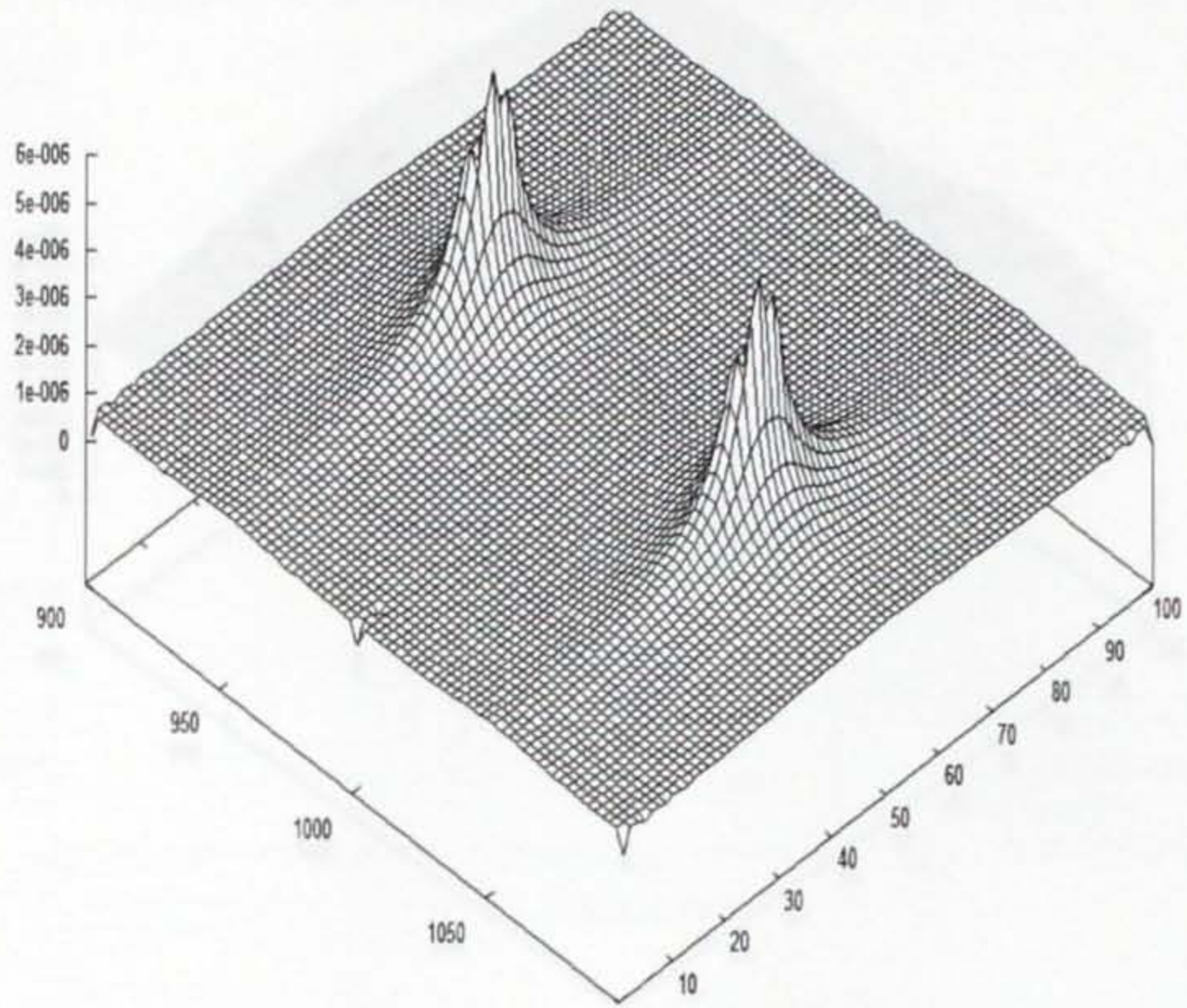
"patch" surrounding the circular cross section of the source. In this patch the wave is propagated using the one-dimensional radial non-linear anelastic wave equation. This is done for several reasons. Firstly it exploits the cylindrical symmetry of the source and the surrounding waves to reduce the dimension of the relevant differential equations by one dimension. Furthermore, it makes the boundary conditions on the cylinder manageable and creates a buffer zone between the region where one-dimensional wave propagation is used and the region of two-dimensional propagation. This makes for a smooth transition when changing from the single radial coordinate r to the rectangular coordinates x and z . Once the patch is fully updated, the simulation proceeds to calculate the wave's propagation in the surrounding region using Cartesian coordinates. Rectangular coordinates are used in this region as they fit the symmetry of the outer boundaries of the grid. Additionally, geophones respond to vertical displacements at the earth's surface and hence it is important to have the z component of the displacement field at the surface of the model.

In altering this code, my work focused on extending the existing framework to allow for multiple sources. This process included a number of stages but can be summarized as follows. First, parameters relating to the patch which were originally scalar variables had to be extended into arrays of length 2. This is done so that the position and other specifications relating to each source could be modified individually. Besides the position of the source, the parameters for each patch default to a common value. The second stage of my work involved editing the update structure of the code. The basic update structure before my modifications involved first updating a single patch and then updating the surrounding grid. After the alteration, each

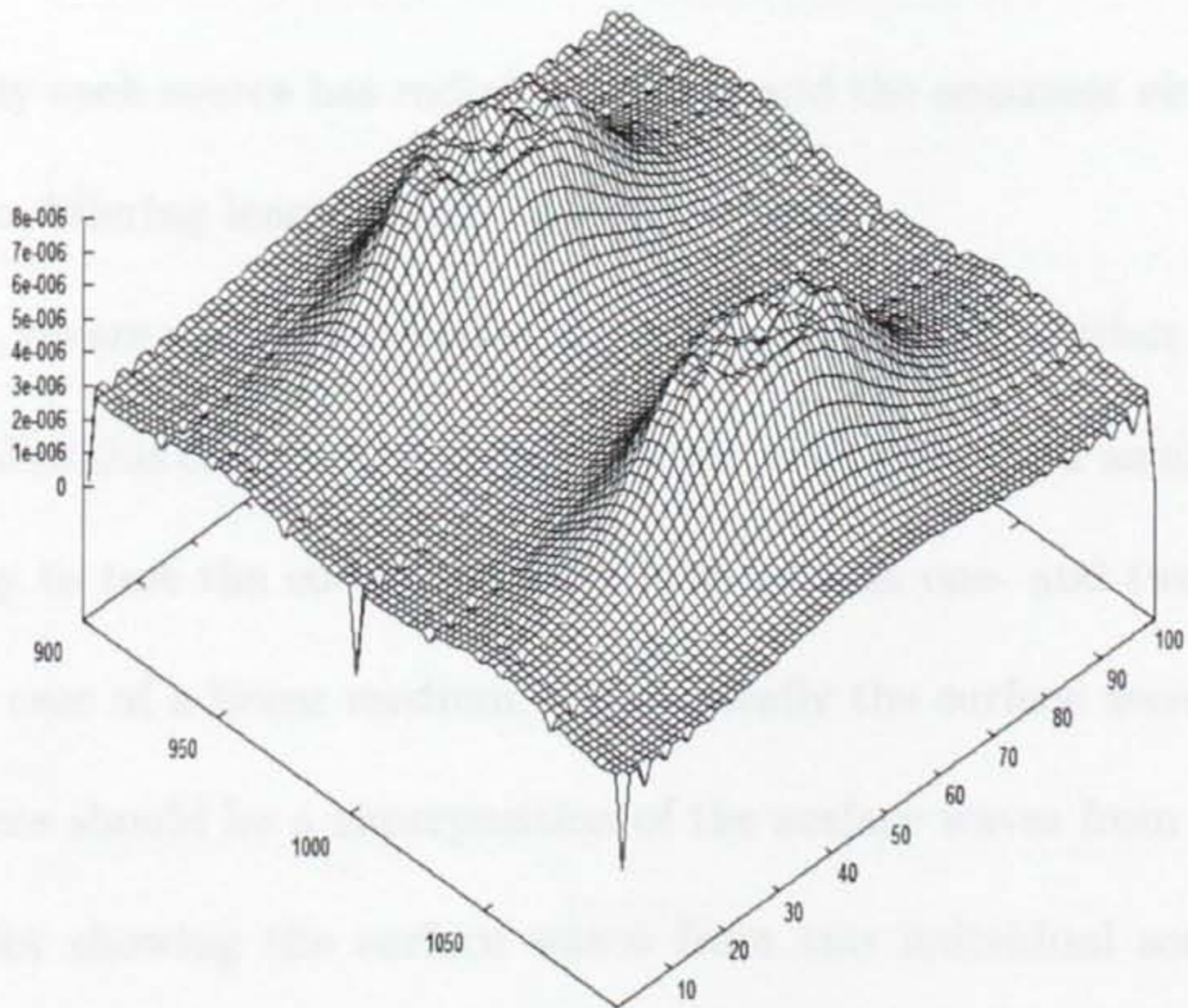
of the two patches were updated and then as before, the rectangular propagation portion of the grid was updated. In making these changes, special care was needed in the placement of the patches. If one patch overlapped the other, then the update from the second patch would effectively "overwrite" the update already completed by the first patch. Conditions forbidding such a situation are checked at the code's onset. If failed, the code stops, preventing wasted time and incorrect output. As a final note, the update of the remaining grid was also altered to accommodate multiple patches. If the original conditions on this update had remained, this step in the update structure would have erased the updates in the region occupied by the second patch.

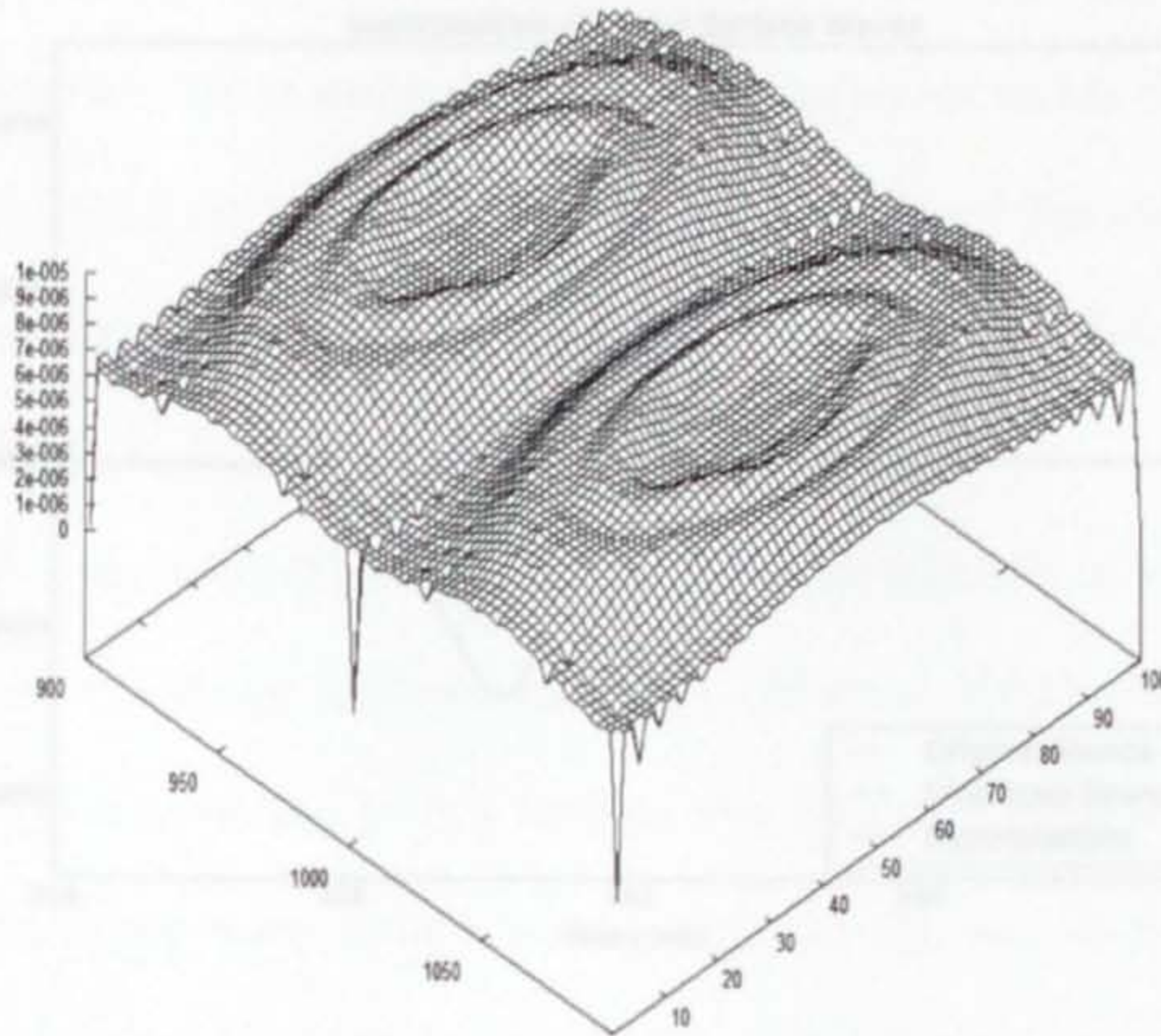
4 Diagnostics, Results, and Future Work

Once the alterations to the simulation were made, it was necessary to make checks that the simulation was in fact giving a reasonable output. In order to get a qualitative picture of the simulation's output, I first looked at the magnitudes of the displacement field as the waves propagated outward. Some figures showing this progression for linear waves are shown below. In each snapshot, the total grid was taken to be 2000 meters wide and 500 meters deep. The sources were placed one hundred meters from one another, both at a depth of 50 meters. The sources were centered at the 1000 meter mark. In each plot the left axis is the length in meters along the horizontal axis while the right axis is the depth in meters. The vertical axis protruding from the page gives the magnitude of the displacement field in meters.



As can be seen, the simulation results are very similar to those from the actual test. In reality, the surface is not smooth, but the simulation results are very smooth. This is due to the fact that the simulation is based on a mathematical model, which is inherently smooth. The actual test results are noisy due to the presence of random noise in the data. The simulation results are therefore a good approximation of the actual test results.



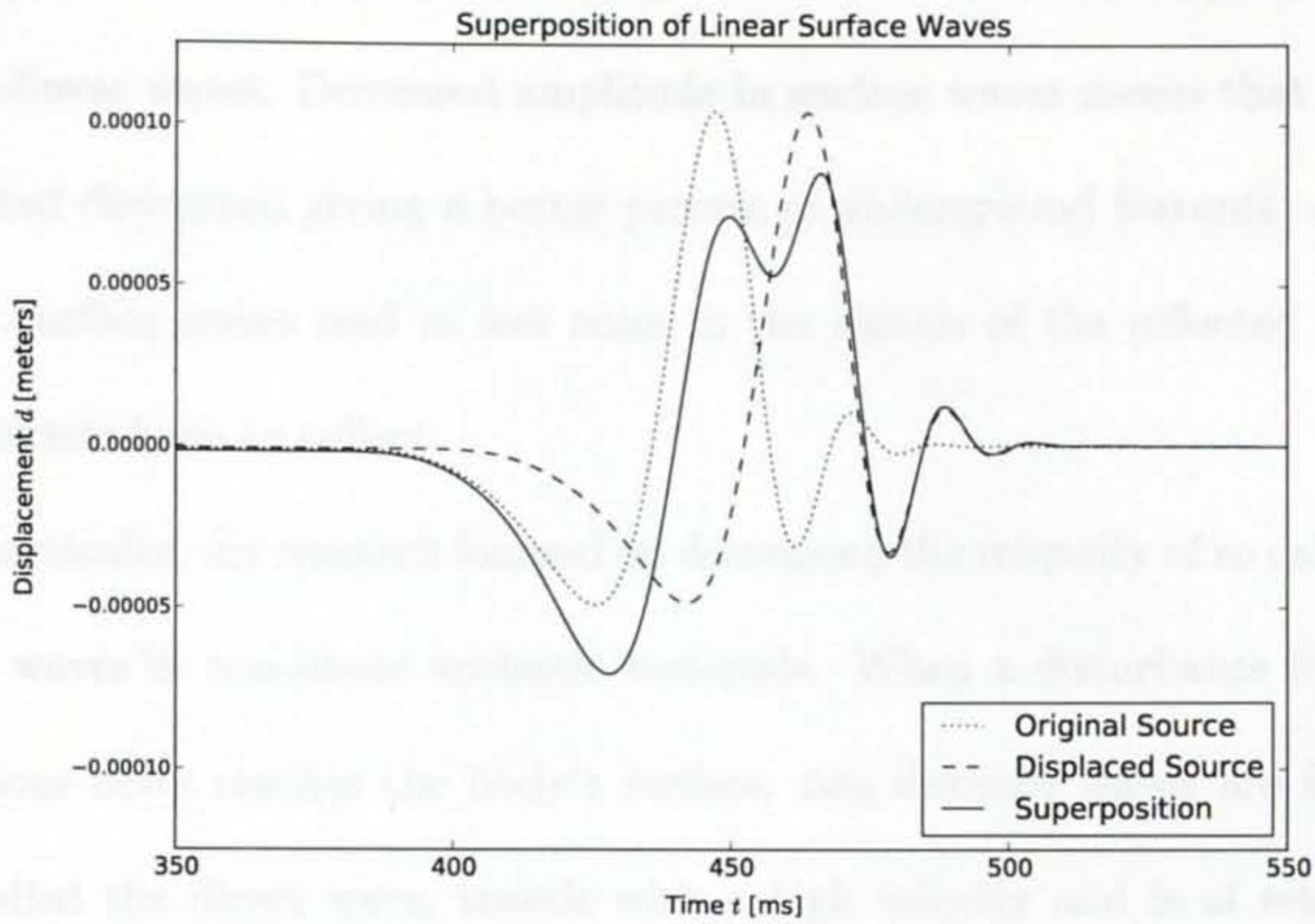


The wave produced by two sources is given as follows. Clearly the wave goes

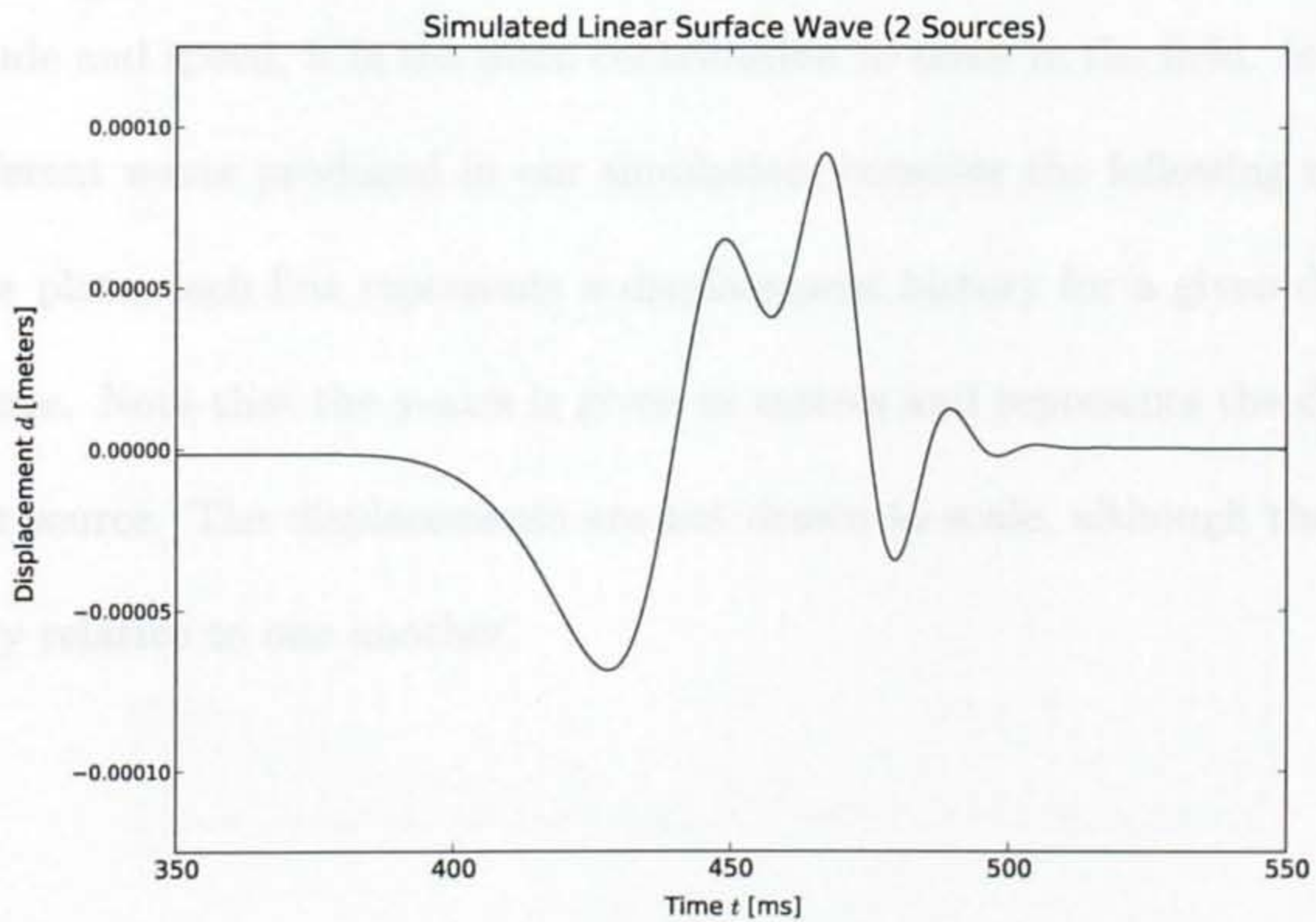
As can be seen, the simulation exhibits reasonable behavior when two sources are used. In reality each source has radial symmetry and the apparent elongation of each wave is due to differing length scales among the axes.

In general, we are most interested in the behavior of the simulation near the surface of the material as this corresponds to the location of geophones in an experiment. One particular way to test the code's accuracy is to look at one- and two-source surface waves for the case of a linear medium. Theoretically the surface wave corresponding to a dual source should be a superposition of the surface waves from each individual source. A plot showing the surface waves from two individual sources and their predicted superposition is given below.

Figure 10: The surface wave from two sources. The left and right panels show the individual surface waves. In addition, there is the predicted superposition of the two waves. The maximum amplitude of the two waves combined is greater than that of either of the



The wave produced by our simulation is given as follows. Clearly the wave pro-



duced by the simulation closely matches the theoretically predicted superposition of individual source waves. In addition, note that in the previous example the maximum amplitude of the two source waveform is smaller than that of either of the

original waves. In this project, we hope to achieve this same type of cancellation for non-linear waves. Decreased amplitude in surface waves means that more energy is directed downward giving a better picture of underground features. Additionally, smaller surface waves lead to less noise in the signals of the reflected waves which geophysicists hope to collect.

In particular, my research focused on decreasing the intensity of so called Rayleigh surface waves in non-linear anelastic materials. When a disturbance from within a continuous body reaches the body's surface, two distance waves are formed. The first, called the direct wave, travels with a high velocity and is of relatively small amplitude. In contrast the second type of wave, called the Rayleigh wave, is of large amplitude and propagates at a much slower speed. Because of the Rayleigh wave's amplitude and speed, it is the main contribution to noise in the field. In order to see the different waves produced in our simulation, consider the following surface plots. In these plots, each line represents a displacement history for a given distance from the source. Note that the y-axis is given in meters and represents the distance from a single source. The displacements are not drawn to scale, although they are scaled properly relative to one another.



Figure 11: Linear waves produced by source at a depth of 10 meters.

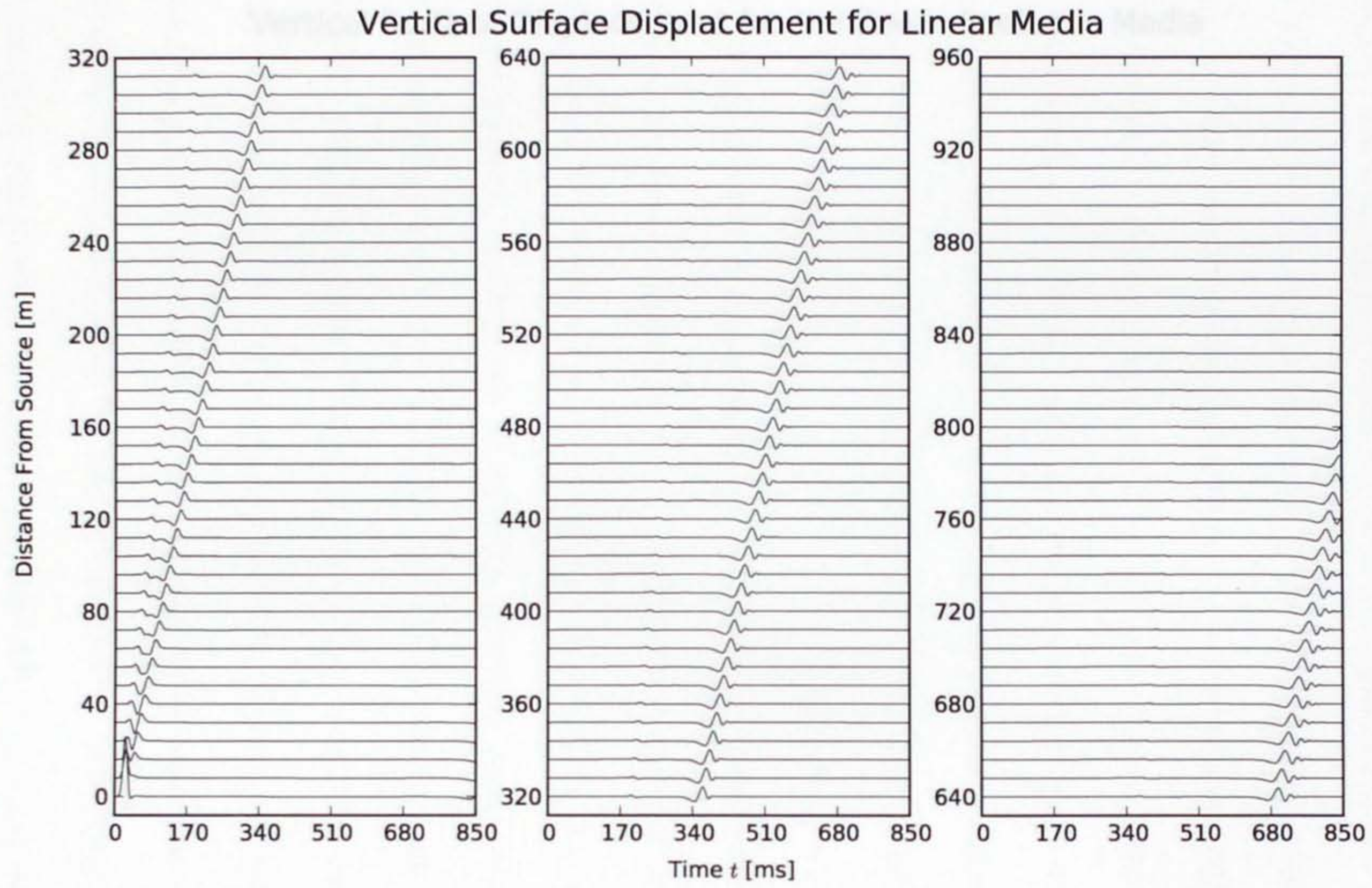


Figure 5: Linear waves produced by source at a depth of 10 meters.

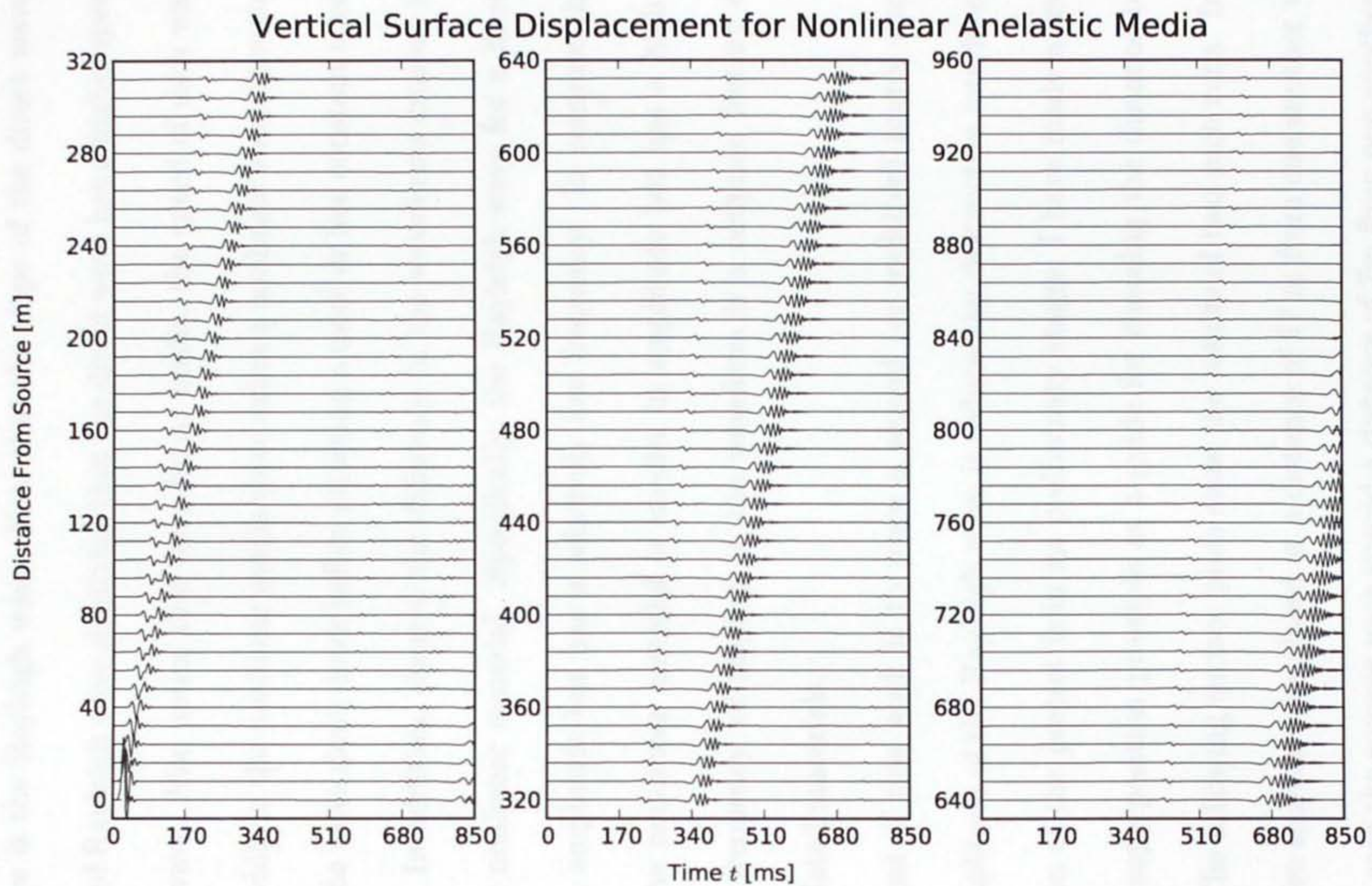


Figure 6: Non-linear waves produced by source at a depth of 10 meters.

In these figures, the small amplitude wave is the direct wave while the large disturbance is the Rayleigh wave. Note that the slope of the direct wave is greater than that of Rayleigh wave signifying that the direct wave has a higher speed than the Rayleigh wave. Also notice that for a linear media, the speed of each wave remains constant while in the nonlinear media there exists a nonlinear zone close to the source in which the wave slows down before attaining a more or less constant speed at larger distances. In addition, observe the difference in the waveforms created in both the linear and nonlinear material. Specifically, the Rayleigh wave for a linear material is large in amplitude but has a relatively low frequency. In contrast the Rayleigh wave in the non-linear material is smaller in amplitude but has a high frequency. This high frequency, or ringing, in the waveform is a common feature observed in unconsolidated materials.

The goal of this work is to place a second (or multiple) source such that the overall amplitude of the Rayleigh wave is reduced by destructive interference. While this portion of the project is in its preliminary stages, I have made a few attempts using the superposition principle as a guide for choosing the distance between the sources. The following surface plots show the results of two such runs. In the linear case the two sources were placed at a distance of 17 m from one another while in the non-linear case the sources were spaced a distance of 7m from one another. As noted earlier, these choices were made using the superposition principle with the hope that it would yield an approximately correct result for the non-linear media.

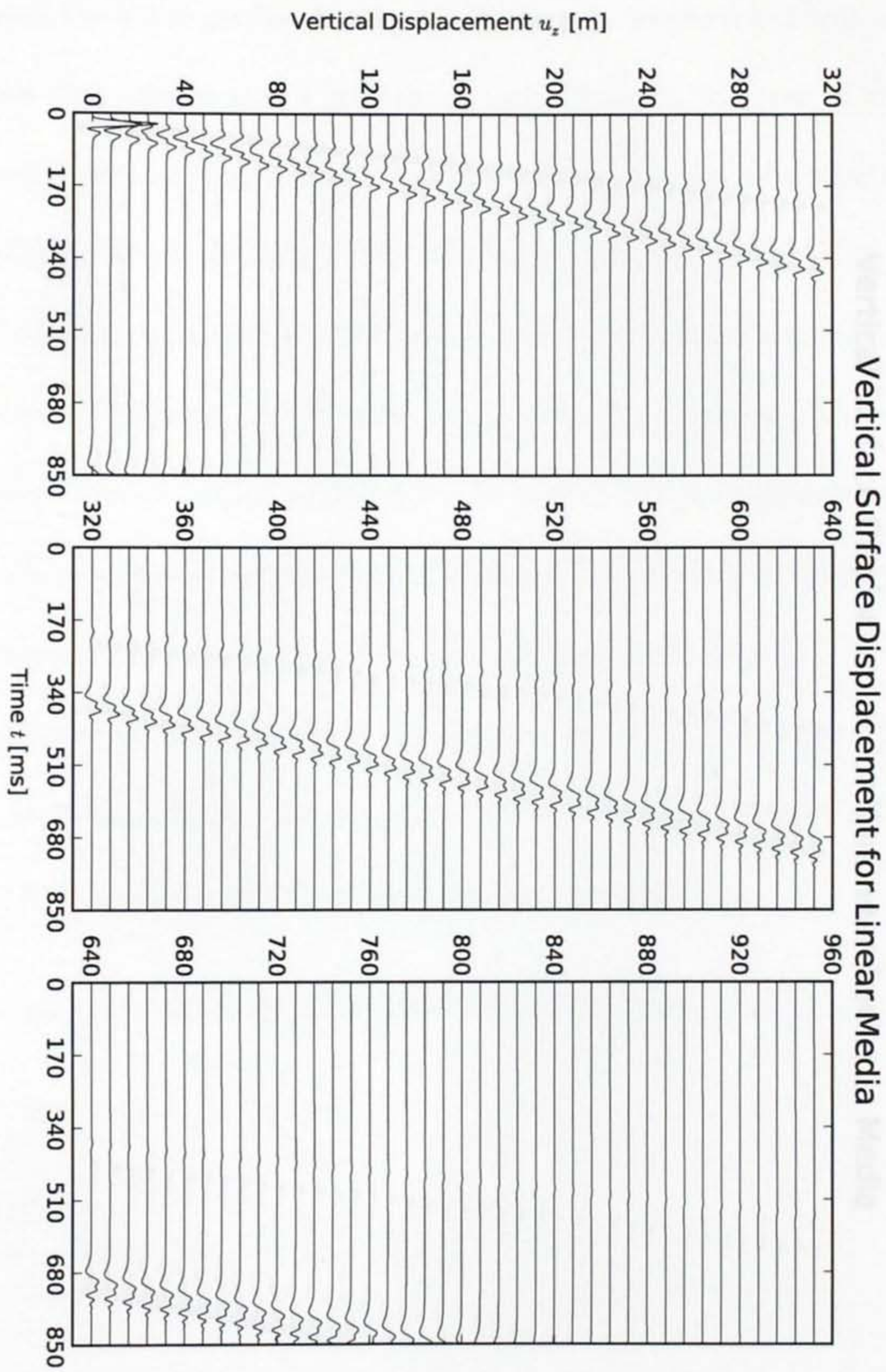


Figure 7: Linear waves produced by dual sources at a depth of 10 meters. One source is placed at the origin of the horizontal coordinates while the other is displaced to -17 meters.

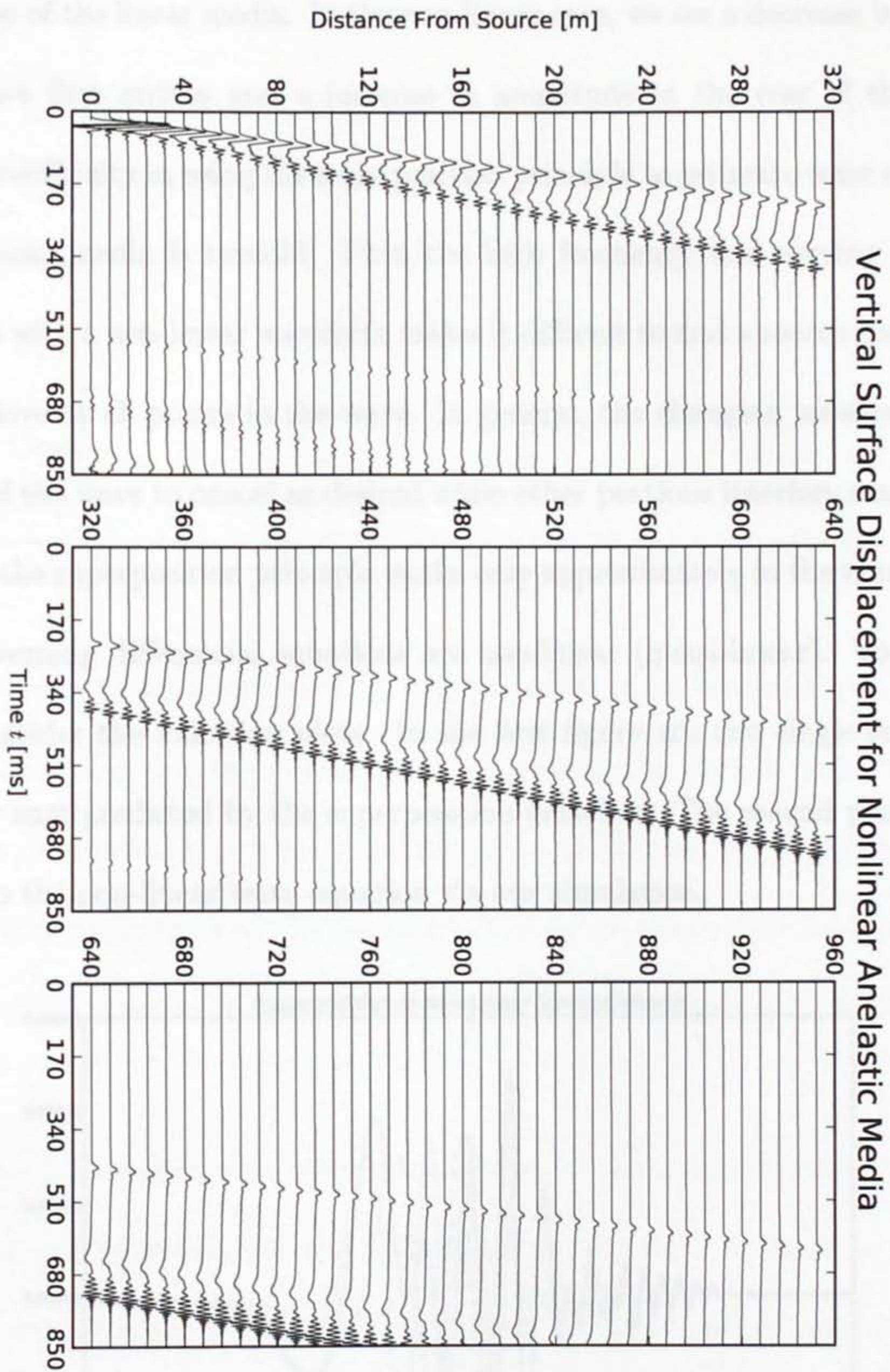
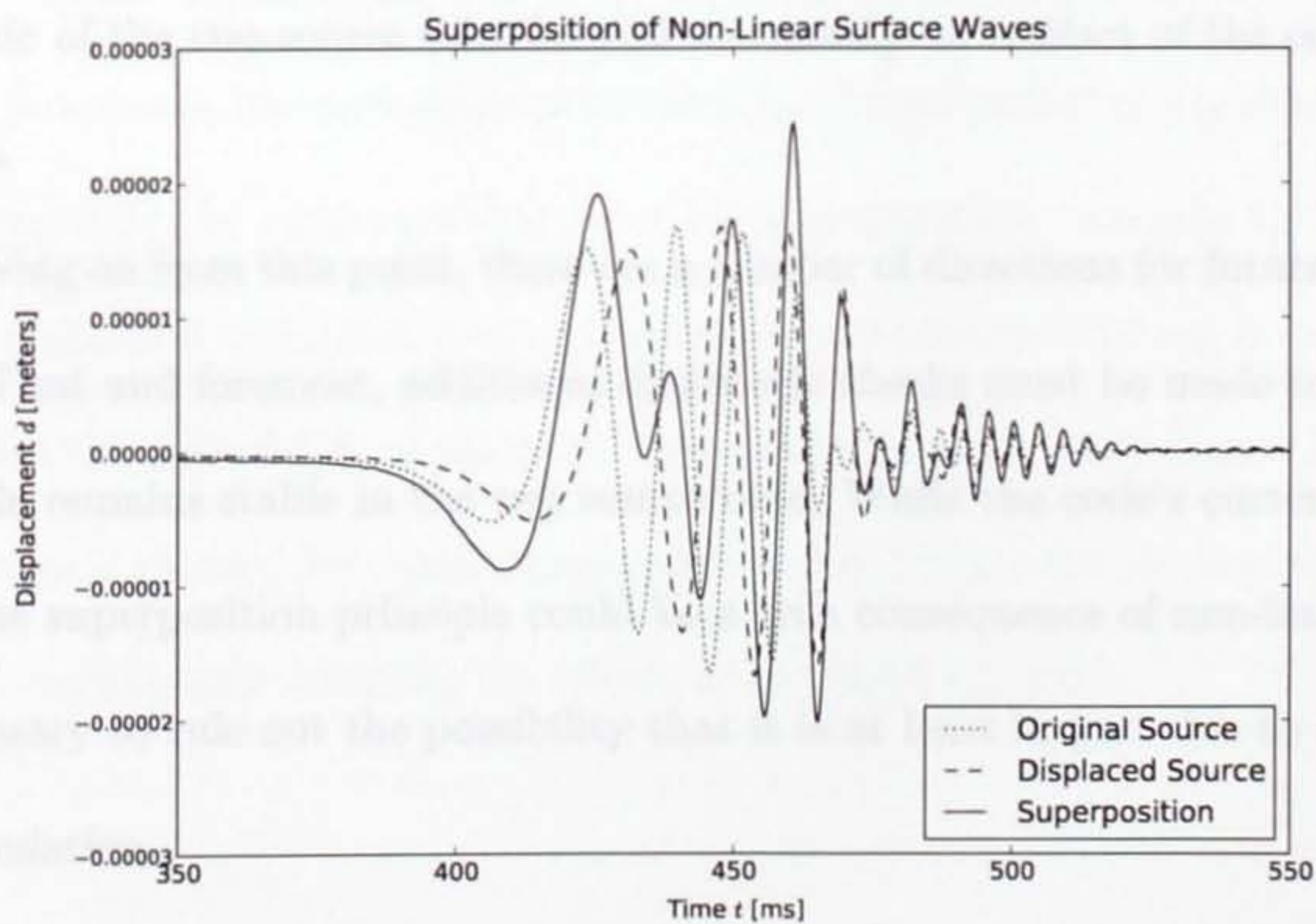
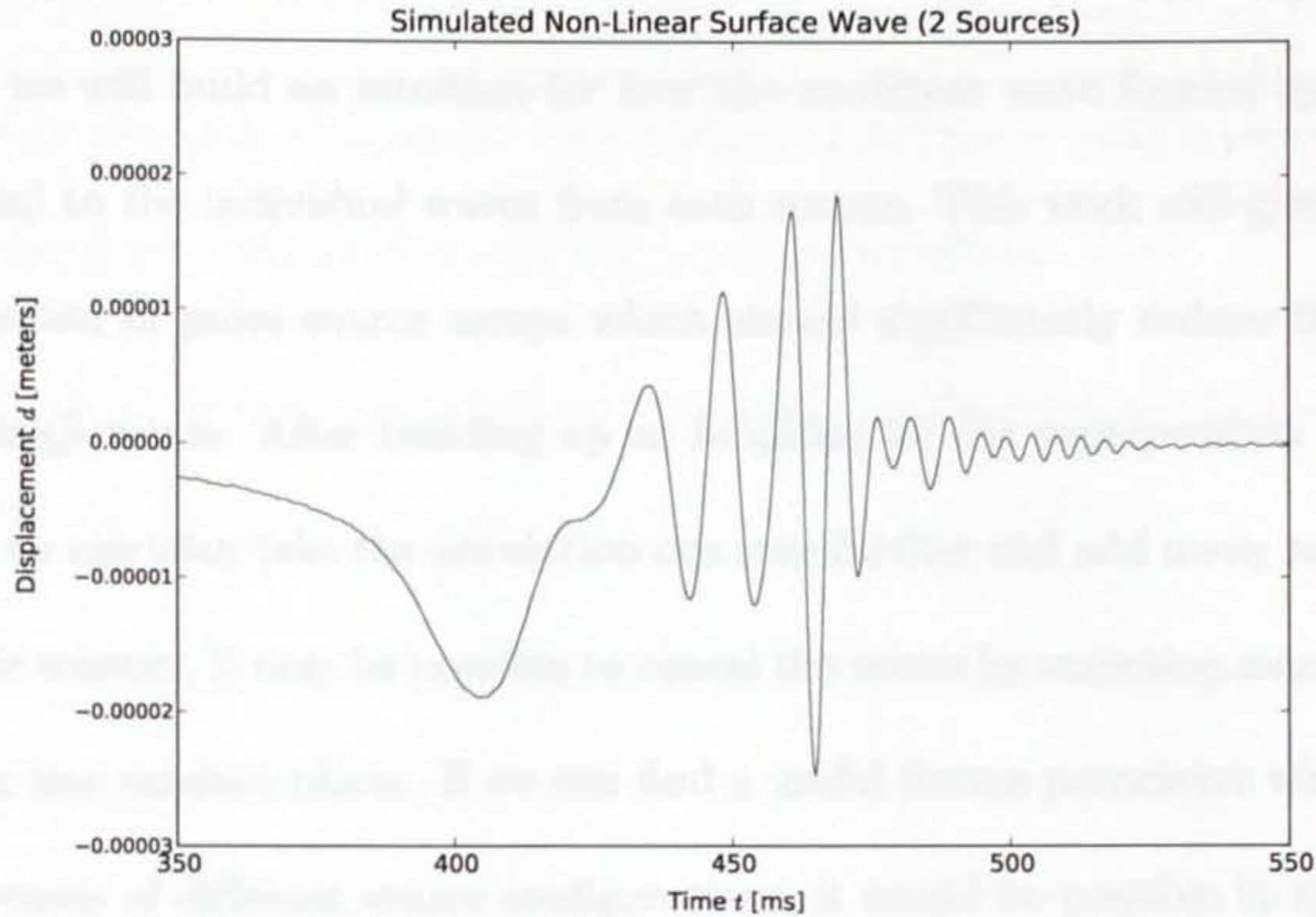


Figure 8: Non-linear waves produced by dual sources at a depth of 10 meters. One source is placed at the origin of the horizontal coordinates while the other is displaced to -7 meters.

Using this technique, the maximum amplitude of the Rayleigh wave was reduced for the case of the linear media. In the non-linear case, we see a decrease in amplitude as the wave first arrives and a increase in amplitude at the rear of the Rayleigh wave. The difficulty in using the superposition principle to estimate wave cancellation for non-linear media is twofold. First the high frequency and varying wavelength associated with a non-linear waveform makes it difficult to find a source spacing which is destructive at all points in the wave. In general, the changing wavelength causes portions of the wave to cancel as desired while other portions interfere constructively. Secondly, the superposition principle works only approximately in the non-linear case as the governing differential equations are non-linear (quasi-linear). To see this in action, consider the following plots. In the first figure are two single source waves with their sum predicted by the superposition principle. The second plot shows the solution to the non-linear wave equation via our simulation.





Clearly, non-linear waves sum in a significantly more complex way than linear waves. Notice both that the peaks do not correspond and that there is a pronounced well which develops at the front of the waveform in between the Rayleigh and direct wave. Further diagnostics will be necessary in order to ensure this behavior is a characteristic of the two-source solution and not merely an artifact of the computational process.

Moving on from this point, there are a number of directions for future work in this topic. First and foremost, additional diagnostic checks must be made to ensure that the code remains stable in the two source case. While the code's current divergence from the superposition principle could be a true consequence of non-linear media, it is necessary to rule out the possibility that it is at least in part due to instability in the simulation.

Once further diagnostics are complete and we have more confidence in the code's

results, additional computational experiments will be performed. Using these experiments we will build an intuition for how the nonlinear wave formed by two sources is related to the individual waves from each source. This work will give guidance in the creation of pulse source arrays which should significantly reduce the amplitude of Rayleigh waves. After building up an intuition for the superposition of non-linear waves, we can then take the simulation one step further and add many sources. Using multiple sources, it may be possible to cancel the waves by summing many waves with more or less random phase. If we can find a useful fitness parameter which rates the effectiveness of different source configurations, it would be possible to systematically scan array designs in search of an optimum design.

In conclusion, this project aimed to address the problem of reducing the amplitude of Rayleigh waves in unconsolidated materials via the interference of multiple source pulses. In accomplishing this task, the non-linear wave propagation simulation created by D.W. Kosik was modified to accommodate multiple pulse sources. In order to assess the modifications, multiple diagnostics were performed including a qualitative analysis of propagation (3d plots) and checks of the superposition principle for linear waves. To date, multiple computational experiments have been carried out in order to probe the behavior of Rayleigh waves in the non-linear multiple source case. In the future, a systematic method for optimizing source pulse design will be developed with the hope of significantly reducing the effects of the Rayleigh wave.

References

- [1] Laura Broaded. Numerical computation of nonlinear wave propagation in two dimensions using the preisach-mayergoyz space model. 2007.
- [2] Milton B. Dobrin. *Introduction to Geophysical Prospecting*. McGraw-Hill, Inc., 1976.
- [3] Y.C. Fung. *A First Course in Continuum Mechanics*. Prentice Hall, Inc., Englewood Cliffs, New Jersey, 1977.
- [4] Russell Gold and Angel Gonzalez. Exxon struggles to find new oil. *The Wall Street Journal*, 2011.
- [5] Oscar Gonzalez and Andrew M. Stuart. *A First Course in Continuum Mechanics*. Cambridge University Press, New York, 2008.
- [6] Robert A. Guyer and Paul A. Johnson. Nonlinear mesoscopic elasticity: Evidence for a new class of materials. *Physics Today*, 53(5):30–36, 1999.
- [7] Robert A. Guyer and Paul A. Johnson. *Nonlinear Mesoscopic Elasticity: The Complex Behaviour of Granular Media including Rocks and Soil*. Wiley, Weinheim, 2009.
- [8] Douglas Heggie and Piet Hut. *The Gravitational Million-Body Problem: A Multidisciplinary Approach to Star Cluster Dynamics*. Cambridge University Press, New York, 2003.

- [9] Dan W. Kosik. Propagation of a nonlinear seismic pulse in an anelastic homogeneous medium. *Geophysics*, 58(7):949–63, 1993.
- [10] D.W. Kosik. Elastodynamic theory.
- [11] I.D. Mayergoyz. Hysteresis models from the mathematical and control theory points of view. *Journal of Applied Physics*, 57(1):3803–5, 1985.
- [12] K.R. McCall and R.A. Guyer. Equation of state and wave propagation in hysteretic nonlinear elastic materials. *Journal of Geophysical Research*, 99(B12):23,887–97, 1994.
- [13] Ivo Sachs, Siddhartha Sen, and James Sexton. *Elements of Statistical Mechanics with an Introduction to Quantum Field Theory and Numerical Simulation*. Cambridge University Press, New York, 2006.
- [14] Lee A. Segel and G.H. Handelman. *Mathematics Applied to Continuum Mechanics*. SIAM, New York, 2007.